Laser and Particle Beams

cambridge.org/lpb

Strong terahertz radiation generation by cosh-Gaussian laser beams in axially magnetized collisional plasma under non-relativistic ponderomotive regime

Prateek Varshney[1], Ajit Upadhayay[1], K. Madhubabu[1], Vivek Sajal[2] and J. A. Chakera[1]

[1]Laser Plasma Section, Raja Ramanna Center for Advance Technology, Indore, Madhya Pradesh-452013, India and [2]Department of Physics and Materials Science and Engineering, Jaypee Institute of Information Technology, Noida, Uttar Pradesh-201307, India

Research Article

Cite this article: Varshney P, Upadhayay A, Madhubabu K, Sajal V, Chakera JA (2018). Strong terahertz radiation generation by cosh-Gaussian laser beams in axially magnetized collisional plasma under non-relativistic ponderomotive regime. *Laser and Particle Beams* **36**, 236–245. https://doi.org/10.1017/S0263034618000216

Received: 11 January 2018
Revised: 3 June 2018
Accepted: 13 June 2018

Key words:
Collisional plasma; cosh-Gaussian beam; rippled plasma; Terahertz radiation

Author for correspondence:
Prateek Varshney, Laser Plasma Section, Raja Ramanna Center for Advance Technology, Indore, Madhya Pradesh-452013, India, E-mail: varshneyprateek28@yahoo.com, varshneyprateek28@gmail.com

Abstract

We propose a scheme for terahertz (THz) radiation generation by non-linear mixing of two cosh-Gaussian laser beams in axially magnetized plasma with spatially periodic density ripple where electron-neutral collisions have been taken into account. The laser beams exert a non-linear ponderomotive force due to spatial non-uniformity in the intensity. The plasma electrons acquire non-linear oscillatory velocity under the influence of ponderomotive force. This oscillatory velocity couples with preformed density ripples ($n' = n_{0\alpha}e^{i\alpha z}$) to generate a strong transient non-linear current that resonantly derives THz radiation of frequency $\sim\omega_h$ (upper hybrid frequency). Laser frequencies (ω_1 and ω_2) are chosen such that the beat frequency (ω) lies in the THz region. The periodicity of density ripple provides phase-matching conditions ($\omega = \omega_1 - \omega_2$ and $\vec{k} = \vec{k_1} - \vec{k_2} + \vec{\alpha}$) to transfer maximum momentum from laser to THz radiation. The axially applied external magnetic field can be utilized to enhance the non-linear coupling and control various parameters of generated THz wave. The effects of decentered parameters (b), collisional frequency (ν_{en}), and magnetic field strength ($B_0 = \omega_c m/e$) are analyzed for strong THz radiation generation. Analytical results show that the amplitude of THz wave enhances with decentered parameters as well as with the magnitude of axially applied magnetic field. The THz amplitude is found to be highly sensitive to collision frequency.

Introduction

In last two decades, the terahertz (THz) radiation in the frequency region 0.1–30 THz has attracted great interest and has become an important area of research in both fundamental and applied sciences. THz radiation has a wide range of applications due to its non-ionizing behavior. Also, it can penetrate in a wide variety of non-conducting materials (Dragoman and Dragoman, 2004). THz radiation sources have a number of applications in the field of spectroscopy (Beard *et al.*, 2002), communication (Bass *et al.*, 1962), remote sensing (Ferguson *et al.*, 2002), THz time-domain spectroscopy (Shen, 2011), sub-millimeter astronomy (Federici *et al.*, 2005), materials characterization (Ferguson and Zhang, 2002), security screening (Federici *et al.*, 2005), tomography (Hu and Nuss, 1995), topography (Wang *et al.*, 2003), and medical diagnostic (Globus *et al.*, 2003; Zeitler *et al.*, 2007). Due to the non-availability of compact and high-power THz radiation sources, the researchers are continuously working toward finding a promising way to generate and tune THz radiation of high amplitude, power, and efficiency with reasonable size.

A variety of schemes are proposed to generate THz from solid-state materials (e.g. electro-optic crystals) such as GaAs, LaTio3, ZnSe, GaP, InP, and $LiNbO_3$ (Kawase *et al.*, 1996; Kadow *et al.*, 2000; Sakai, 2005). The low damage threshold of these materials, low conversions efficiency, and narrow band width make it difficult to generate high-power, highly efficient, and tunable THz sources using them. Due to these disadvantages, in last few years, a lot of investigations have been carried out to introduce new schemes for THz generation. Plasma, being a broken medium, has no damage threshold and can handle very high-power laser beam. Hence, several laser–plasma interactions-based schemes (experimentally and theoretically) have been proposed by researchers for high-power THz radiation sources (Hamster *et al.*, 1993, 1994; Cook and Hochstrasser, 2000; Löffler *et al.*, 2000; Carr *et al.*, 2002; Dai *et al.*, 2006; Biedron *et al.*, 2007; Liu *et al.*, 2007; Houard *et al.*, 2008; Kim *et al.*, 2008; Liu and Tripathi, 2009; Malik *et al.*, 2010, 2017; Tripathi *et al.*, 2010; Malik and Malik, 2012; Singh *et al.*, 2012; Nafil *et al.*, 2013; Mondal *et al.*, 2017; Wang *et al.*, 2017).

CAMBRIDGE UNIVERSITY PRESS

THz generation using laser filamentation, self-focusing, cross-focusing, and photoionization in plasma using highly intense ultra-short picosecond or a femtosecond range laser pulses have been performed by several researchers (Carr *et al.*, 2002; Dai *et al.*, 2006; Biedron *et al.*, 2007; Houard *et al.*, 2008; Kim *et al.*, 2008). Chen *et al.* (2007) have reported that THz generation experiment in laser produced plasma from a series of noble gases. They have shown that the THz efficiency increases with decreasing ionization potential. Hamster *et al.* (1993) experimentally demonstrated THz radiation from short-pulse laser beam focused on gas and solid targets. They also examined THz radiation in laser-induced plasma channel where ponderomotive force drives THz radiation (Hamster *et al.*, 1994). Babushkin *et al.* have studied numerically (Babushkin *et al.*, 2010b) and experimentally (Babushkin *et al.*, 2010a) the THz radiation in air and noble gas by two color lasers in an ionizing plasma using 0.8 and 1.6 μm laser of 50 fs duration.

The analytical investigation of the THz radiation generation by non-linear mixing of two laser beams in plasma having their frequency differences in THz region have been studied by many researchers in the last few years (Bhasin and Tripathi, 2009; Liu and Tripathi, 2009; Pathak *et al.*, 2009; Kumar *et al.*, 2010, 2017; Malik *et al.*, 2010, 2017; Sharma *et al.*, 2010; Malik and Malik, 2011, 2013; Varshney *et al.*, 2013, 2015a, 2015b, 2017; Malik, 2014, 2015; Sharma and Singh, 2014; Singh and Sharma, 2014; Varshnety *et al.*, 2014; Bakhtiari *et al.*, 2015a, 2015b, 2017; Gill *et al.*, 2017; Rawat *et al.*, 2017; Singh *et al.*, 2017). Cho *et al.* (2015) have demonstrated a new mechanism for THz generation based on laser–plasma interaction. They have shown that a monochromatic THz radiation with a field strength of $\sim 10^7$ V/m can be produced by two counter propagating short laser pulse in weakly magnetized plasma. THz radiation by laser–plasma interaction in rippled plasma density has been studied by many researchers. Its role in the generation process has been examined and discussed in detail (Bhasin and Tripathi, 2009; Pathak *et al.*, 2009; Tripathi *et al.*, 2010; Varshney *et al.*, 2013, 2017). Antonsen Jr *et al.* (2007) have analytically studied phase-matched THz radiation generation by the ponderomotive force of a laser pulse with the employment of a corrugated plasma channel. In another analytical study, Bhasin and Tripathi (2009) have obtained THz radiation with an efficiency of 10^{-4} by the optical rectification of an *x*-mode picosecond laser pulse in a rippled density magnetized plasma. Their model was further improved by Varshney *et al.* (2013) by including the effects of the static magnetic field on ponderomotive force.

Various laser profiles, for example, Gaussian (Bhasin and Tripathi, 2009; Malik *et al.*, 2010; Singh and Sharma, 2014), triangular (Malik *et al.*, 2011; Varshney *et al.*, 2015a), cosh-Gaussian (Singh *et al.*, 2013; Mann *et al.*, 2017; Varshney *et al.*, 2017), super-Gaussian (Malik *et al.*, 2010; Malik and Malik, 2012; Varshney *et al.*, 2015b), and flat-top (Bakhtiari *et al.*, 2017) have been used to generate strong and tunable THz radiation because laser beams with different intensity profiles behave differently in plasmas. For example, Malik *et al.* have utilized the super-Gaussian (Malik and Malik, 2012), Gaussian (Malik *et al.*, 2012), and spatial triangular (Malik *et al.*, 2011) profiles of beating lasers in a periodic density rippled plasma for THz generation and obtained a maximum efficiency of about 10^{-2} for the laser intensity of 10^{14} W/cm^2. They have also shown that stronger THz radiation can be produced with the help of two spatial super-Gaussian lasers of higher index and smaller beam width (Malik and Malik, 2012). Singh *et al.* (2013) have obtained THz radiation with an efficiency of 10^{-5} by beating of two cosh-Gaussian laser beams in spatially periodic density plasma. This model has been further improved by Varshney *et al.* (2017) by including the effects of the static magnetic field in the plasma where they have shown three-order higher efficiency.

In most of the THz radiation generation schemes mentioned earlier, the electron-neutral collisions in plasma has not been taken into account as it leads to drastic reduction in the emitted THz power and efficiency. Also, the joint effects of the collisions and the magnetic fields have not been considered. Singh and Malik (2015) have considered the effects of collisional plasma for THz radiation generation by mixing two super-Gaussian laser beams. They have shown that electron-neutral collision and larger beam width lead to significant change in THz amplitude. But when super-Gaussian laser is used in plasma, the efficiency of mechanism remains much higher than the case of Gaussian lasers. They have also studied the effect of magnetic field and demonstrated 6% efficiency (Singh and Malik, 2014). Recently, generation of THz radiation by hollow-Gaussian laser beams in collisional plasmas has been studied by Bakhtiari *et al.* (2015a) where they observed the efficiency of THz radiation is very small, which is due to the collisional effect. By considering the interaction of two flat-topped laser profiles, Bakhtiari *et al.* (2017) demonstrated an efficiency of THz generation of 8.3% in a collisional plasma.

In this work, we study THz radiation generation by beating of two coaxial cosh-Gaussian laser beams propagating in rippled density magnetized plasma in the presence of applied axial static magnetic field. The cosh-Gaussian beams (decentered Gaussian beams) have raised considerable interest in recent times on account of their spatial profile. These beams control higher efficient power with flat-top beam shape and hollow-Gaussian lasers beam in comparison with that of a Gaussian beam. Contrary to the case of two Gaussian spatial profile lasers, THz radiation can be focused at a desired position by choosing suitable decentered parameters of cosh-Gaussian lasers (Varshney *et al.*, 2017). We show that in magnetized plasma, if the effect of electron-neutral collisions is taken into account, THz radiation enhances significantly in terms of the amplitude and efficiency. In a specific parameter domain, the joint effect of the magnetic field and electron-neutral collisions causes enhancement of THz amplitude and efficiency. Optimizing the plasma and laser beam parameters and considering the mutual effect, we obtain the efficiency of THz generation up to 15%, which is considerably high relative to the efficiency obtained in the previously studied schemes. In "Calculation of nonlinear current density, THz radiation field amplitude and efficiency" section, we develop the analytical model of THz radiation in collisional and magnetized plasma, and equations for the emitted THz field amplitude and efficiency are then derived. The results of the numerical study are presented and discussed in "Analytical result and discussion" section. Finally, "Conclusions" section contains conclusion.

Calculation of non-linear current density, THz radiation field amplitude, and efficiency

We consider two circular symmetric cosh-Gaussian laser beams with different frequencies (ω_1 and ω_2) and wave numbers ($\vec{k}_1$ and $\vec{k}_2$) co-propagating along *z*-axis in the collisional plasma (electron-neutral collisions). A static magnetic field B_0 is applied along the direction of wave propagation. The profile of laser

https://doi.org/10.1017/S0263034618000216 Published online by Cambridge University Press

electric fields is given as

$$\vec{E}_j = (\hat{x}E_{0jx} + \hat{y}E_{0jy})\cosh\left(\frac{rb}{r_0}\right)e^{-y^2/r_0^2}e^{-i(\omega_j t - k_j z)}, \quad (1)$$

where

$$E_{0jx} = E_{0jy} = E_{0j}. \quad (2)$$

Here, $k_j = (\omega_j/c)\{1-(\omega_p^2/\omega_j(\Omega_j-\omega_c))\}^{1/2}$, $j = 1,\ 2$ for two lasers and $\Omega_j = \omega_j - i\upsilon_{en}$. Here, $\omega_p = (4\pi n_{0e}e^2/m)^{1/2}$ is the plasma frequency (in CGS), cyclotron frequency $\omega_c = eB_0/mc$ (in CGS), υ_{en} is the collisional frequency, r_0 is the initial beam width, b is the decentered parameter, e is the electronic charge, and m is the electronic mass. The electric field profile given by Eq. (1) is plotted in Figure 1. One can notice that as decentered parameter of the cosh-Gaussian laser beam changes from $b = 0$ to 5, the profile changes its shape in the following sequences: (i) Gaussian ($b = 0$), (ii) flat-top ($b = 1.45$), (iii) ring shape ($b = 2$), and (iv) hollow-Gaussian ($b = 5$).

The plasma has a periodic density ripple given by $n = n_0 + n'$, $n' = n_{\alpha 0}e^{i\alpha z}$, where $n_{\alpha 0}$ is the amplitude of ripple and α is the repetition factor for density ripples. This density ripple may be created using various techniques, for example, by machining prepulse and a patterned mask, where plasma gas jet is exposed to an ultrahigh-intensity laser pulse through a patterned mask of periodic opacity. Hydrodynamics expansions, in the irradiated regions exposed to higher intensity part of laser, are created due to heating by the laser pulse and plasma density drops in this region. Thus, a masked laser beam can be utilized to pre-form the spatially periodic ripple density structure in the plasma. Here, one can control ripple parameters ($n_{\alpha 0}$ and α) by changing the size of the masks (Pai *et al.*, 2005). Taking in to account the electron-neutral collisions, the equation of motion for laser beams can be written as (Chen and Trivelpiece, 1976):

$$m\frac{d\vec{v}_j}{dt} = -e\vec{E}_j - e(\vec{v}_j \times \vec{B}_j) - m\upsilon_{en}\vec{v}_j. \quad (3)$$

The last term in Eq. (3) represents the collisional force. Plasma electron oscillates under the influence of electric field of beating lasers and attains oscillating velocities having $\hat{x}$ and $\hat{y}$ components, given by

$$v_{jx} = \frac{eE_{jx}\Omega_j}{mi(\Omega_j^2-\omega_c^2)} - \frac{eE_{jy}\omega_c}{m(\Omega_j^2-\omega_c^2)}, \quad (4a)$$

$$v_{jy} = \frac{eE_{jy}\Omega_j}{mi(\Omega_j^2-\omega_c^2)} + \frac{eE_{jx}\omega_c}{m(\Omega_j^2-\omega_c^2)}. \quad (4b)$$

Two lasers beating at frequency $\omega = \omega_1 - \omega_2$ and wave vector $\vec{k} = \vec{k}_1 - \vec{k}_2$ create a non-linear ponderomotive force $\vec{F}_p^{NL}$ on plasma electrons, which is given by:

$$\vec{F}_p^{NL} = -\frac{m\nabla\vec{v}_1.\vec{v}_2^*}{2}. \quad (5)$$

The non-linear ponderomotive force is evaluated using Eq. (4) and becomes

$$\vec{F}_p^{NL} = \frac{e^2}{m(\Omega_1-\omega_c)(\Omega_2^*-\omega_c)} \nabla\left[\cosh^2\left(\frac{rb}{r_0}\right)\times\exp\left(-\frac{2r^2}{r_0^2}\right)\right]\exp\left(-i(\omega t - k'z)\right). \quad (6)$$

This non-linear ponderomotive force causes perturbations in the density of plasma ($n = n^L + n^{NL}$) having linear component and non-linear component. These perturbations generate space charge potentials that lead to the linear density perturbation. The non-linear density perturbation is due to the non-linear ponderomotive force. This non-linear force imparts non-linear oscillatory velocity to the electrons, which is calculated by the equation of motion:

$$m\frac{\partial\vec{v}_{NL}}{\partial t} = F_p^{NL} - \frac{e}{c}(\vec{v}^{NL}\times\vec{B}_0) - m\upsilon_{en}\vec{v}^{NL}. \quad (7)$$

Here, we have taken into account only electron-neutral collisions. On solving Eq. (7), we obtain the value of non-linear velocity component as follows:

$$v_x^{NL} = \frac{-i\omega_c F_{py}^{NL} + \Omega F_{px}^{NL}}{m\,i(\Omega^2-\omega_c^2)}, \quad (8a)$$

$$v_y^{NL} = \frac{i\omega_c F_{px}^{NL} + \Omega F_{py}^{NL}}{m\,i(\Omega^2-\omega_c^2)}. \quad (8b)$$

This oscillatory velocity couples with preformed density ripple $n_{\alpha 0}e^{i\alpha z}$ and excites a non-linear current density at $(\omega,\ \vec{k}_1 - \vec{k}_2 + \vec{\alpha})$, which can be written as

$$\vec{J}^{NL} = -\frac{1}{2}n_{\alpha 0}e\vec{v}^{NL}e^{i\alpha z}. \quad (9)$$

The above equation shows that a non-linear transverse current is formed. This current may lead to radiation at different frequencies $\omega = \omega_1 - \omega_2$ and wave numbers $\vec{k}(= \vec{k}_1 - \vec{k}_2 + \vec{\alpha})$. The value of ω and k may be chosen such that the generated radiation lies in the THz region. Using Maxwell's equations, the wave equation governing the propagation of THz radiation in axially magnetized plasma can be written as:

$$\nabla^2\vec{E}_{THz} - \vec{\nabla}(\vec{\nabla}.\vec{E}_{THz}) + \frac{\omega^2}{c^2}(\bar{\bar{\varepsilon}}\,\vec{E}_{THz}) = -\frac{4\pi i\omega}{c^2}\vec{J}^{NL}, \quad (10)$$

where, $\bar{\bar{\varepsilon}}$ is the plasma permittivity tensor at ω and its components are $\varepsilon_{xx} = \varepsilon_{yy} = \left[1-(\omega_p^2\Omega/\omega(\Omega^2-\omega_c^2))\right]$, $\varepsilon_{xy} = -\varepsilon_{yx} = \frac{i\omega_c\omega_p^2}{\omega(\Omega^2-\omega_c^2)}$, $\varepsilon_{zz} = \left[1-(\omega_p^2/\omega\,\Omega)\right]$, and $\varepsilon_{xz} = \varepsilon_{yz} = \varepsilon_{zx} = \varepsilon_{zy} = 0$. We wish to emphasize here that the transverse components of non-linear current density are the source of THz radiation generation. We can separate out the transverse

https://doi.org/10.1017/S0263034618000216 Published online by Cambridge University Press

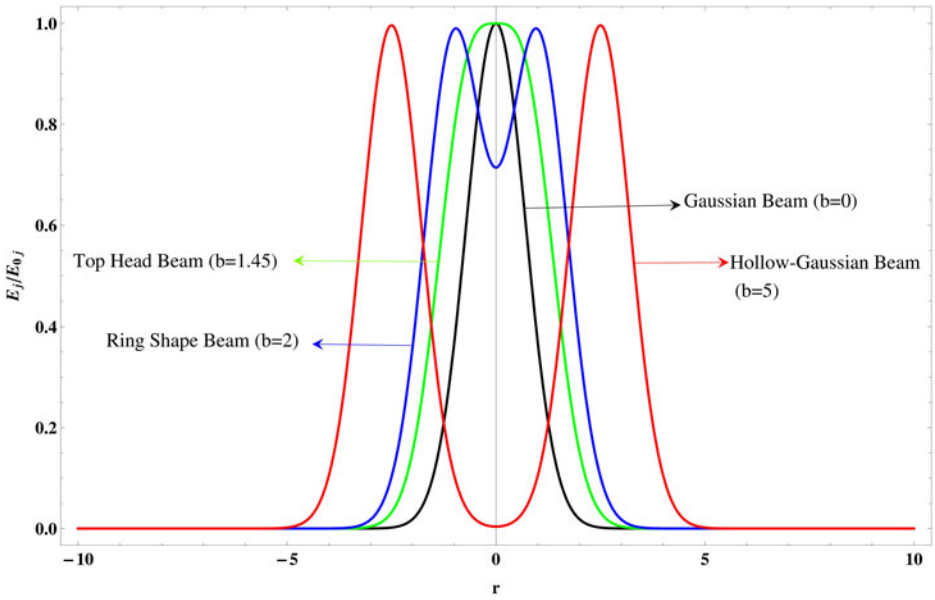

Fig. 1. Normalized cosh-Gaussian laser field amplitude E_j/E_{0j} as a function of transverse distance r for decentered parameters $0 < b \leq 5$.

components of Eq. (10) as follows:

$$\nabla^2 E_{x\mathrm{THz}} - \frac{\partial}{\partial x}(\vec{\nabla}.\vec{E}_{\mathrm{THz}}) + \frac{\omega^2}{c^2}(\varepsilon_{xx}E_{x\mathrm{THz}} + \varepsilon_{xy}E_{y\mathrm{THz}}) = -\frac{4\pi i\omega}{c^2}J_x^{\mathrm{NL}} \tag{11}$$

and

$$\nabla^2 E_{y\mathrm{THz}} - \frac{\partial}{\partial y}(\vec{\nabla}.\vec{E}_{\mathrm{THz}}) + \frac{\omega^2}{c^2}(\varepsilon_{yx}E_{x\mathrm{THz}} + \varepsilon_{yy}E_{y\mathrm{THz}}) = -\frac{4\pi i\omega}{c^2}J_y^{\mathrm{NL}}. \tag{12}$$

We multiply Eq. (12) by i and subtract it from Eq. (11) and also use Eq. (2) to obtain

$$\nabla^2 E_{x\mathrm{THz}} - \frac{1}{2}\left[\left(\frac{\partial}{\partial x} - i\frac{\partial}{\partial y}\right)(\vec{\nabla}.\vec{E}_{\mathrm{THz}})\right] + \frac{\omega^2}{c^2}(\varepsilon_{xx} + i\varepsilon_{xy})E_{x\mathrm{THz}} = -\frac{4\pi i\omega}{c^2}(J_x^{\mathrm{NL}} - iJ_y^{\mathrm{NL}}). \tag{13}$$

Taking fast-phase variations in the electric field of THz radiation as $E_{x\mathrm{THz}} = E_{0\,\mathrm{THz}}\exp\{-i(\omega t - kz)\}$ and neglecting second-order perturbations of Eq. (13), we can write Eq. (13) as:

$$2ik\frac{\partial}{\partial z}E_{0\,\mathrm{THz}} + \left(\frac{\omega^2}{c^2}(\varepsilon_{xx} + i\varepsilon_{xy}) - k^2\right)E_{0\,\mathrm{THz}} = \frac{4\pi i\omega}{c^2}(J_x^{\mathrm{NL}} - iJ_y^{\mathrm{NL}}). \tag{14}$$

The resonance condition of phase matching in the presence of periodic plasma density ripple demands that the second term on left-hand side of Eq. (14) is equal to zero. This leads to the dispersion relation of THz.

$$k^2 = \frac{\omega^2}{c^2}(\varepsilon_{xx} + i\varepsilon_{xy}) = \frac{\omega^2}{c^2}\left(1 - \frac{\omega_{\mathrm{p}}^2}{\omega(\Omega - \omega_{\mathrm{c}})}\right). \tag{15}$$

This second term on left-hand side of Eq. (14) suggests that the maximum energy transfer from beating lasers to oscillating electron current leading to THz radiation will take place at resonance condition $\vec{k} = \vec{k}_1 - \vec{k}_2 + \alpha$ and $\omega = \omega_1 - \omega_2 \approx \omega_{\mathrm{h}}$. The periodicity of density ripples required for the fine tuning of maximum energy transfer is calculated utilizing Eq. (15) as follows:

$$\alpha = \frac{\omega}{c}\left|\left(1 - \frac{\omega_{\mathrm{p}}^2}{\omega(\Omega - \omega_{\mathrm{c}})}\right)^{1/2} - 1\right|. \tag{16}$$

On recombining Eqs. (8), (9), (14), and (16), we obtain the phase-matched THz wave amplitude:

$$E_{0\,\mathrm{THz}} = \frac{n_{\alpha 0}}{n_0}\frac{\omega_{\mathrm{p}}^2\omega\, zeE_{01}E_{02}^*\exp(-2r^2/r_0^2)}{8mikc^2(\omega_{\mathrm{c}} - \omega)(\Omega_1 - \omega_{\mathrm{c}})(\Omega_2^* - \omega_{\mathrm{c}})}\left[\frac{-2r}{r_0^2} + \frac{2b}{r_0}\sinh\left(\frac{2rb}{r_0}\right) + \frac{4r}{r_0^2}\cosh\left(\frac{2rb}{r_0}\right)\right]. \tag{17}$$

Normalizing Eq. (17), we obtain final expression of the normalized amplitude of THz wave as follows:

$$\left|\frac{E_{0\mathrm{THz}}}{E_{01}}\right| = \frac{n_{\alpha 0}}{n_0}\frac{\omega' z'\left|v_{02}'^*\right|\exp(-2r'^2/r_0'^2)}{8k'(\omega_{\mathrm{c}}' - \omega')(\Omega_1' - \omega_{\mathrm{c}}')(\Omega_2'^* - \omega_{\mathrm{c}}')}\left[\frac{-2r'}{r_0'^2} + \frac{2b}{r_0'}\sinh\left(\frac{2r'b}{r_0'}\right) + \frac{4r'}{r_0'^2}\cosh\left(\frac{2r'b}{r_0'}\right)\right], \tag{18}$$

where $z' = z\omega_{\mathrm{p}}/c$, $\Omega_1' = \Omega_1/\omega_{\mathrm{p}}$, $\Omega_2'^* = \Omega_2^*/\omega_{\mathrm{p}}$, $r_0' = r_0\omega_{\mathrm{p}}/c$, $\omega'_{\mathrm{c}} = \omega_{\mathrm{c}}/\omega_{\mathrm{p}}$, $\omega = \omega/\omega_{\mathrm{p}}$, $k' = kc/\omega_{\mathrm{p}}$, and $r' = r\omega_{\mathrm{p}}/c$.

The efficiency of the emitted THz radiation can be calculated by the ratio of the THz radiation energy and the incident laser

https://doi.org/10.1017/S0263034618000216 Published online by Cambridge University Press

energy. The average electromagnetic energy stored per unit volume in electric and magnetic fields are given by the relations (Rothwell and Cloud, 2008; Varshney *et al.*, 2015b).

$$\langle W_{,i}\rangle = \frac{1}{8\pi}\varepsilon_0 \frac{\partial}{\partial \omega_i}\left[\omega_i\left(1-\frac{\omega_p^2}{\omega_i^2}\right)\right]\langle |E_i|^2\rangle, \tag{19a}$$

$$\langle W_{B_i}\rangle = \frac{k^2}{8\pi\mu_0\omega_i}\langle |E_i|^2\rangle. \tag{19b}$$

The energy densities of the incident lasers (W_{pump}) and emitted radiation (W_{THz}) are as follows:

$$W_{\text{pump}} = \frac{\varepsilon_0 r'_0}{2}|E_{01}|^2\sqrt{\frac{\pi}{2}}\left\{1+\exp\left[\frac{b^2}{2}\right]\right\}, \tag{20}$$

$$W_{\text{THz}} = \varepsilon_0|E_{01}|^2\left[\frac{n_{\alpha 0}}{n_0}\frac{\omega' z'\left|v'^*_{02}\right|}{16k' r'_0(\omega'_c-\omega')(\Omega'_1-\omega'_c)(\Omega'^*_2-\omega'_c)}\right]$$
$$\left[1+2b\,e^{b^2/2}\sqrt{2\pi}\,Erf\left(\frac{b}{\sqrt{2}}\right)\right]. \tag{21}$$

The normalized efficiency of THz radiation generation can be evaluated as follows:

$$\eta_{\text{THz}} = \frac{W_{\text{THz}}}{W_{\text{pump}}} = \sqrt{\frac{2}{\pi}}\frac{n_{\alpha 0}}{n_0}\frac{\omega' z'\left|v'^*_{02}\right|}{8k' r'^2_0(\omega'_c-\omega')(\Omega'_1-\omega'_c)(\Omega'^*_2-\omega'_c)}$$
$$\left[\frac{1+2b\,e^{b^2/2}\sqrt{2\pi}\,Erf\left(b/\sqrt{2}\right)}{1+\exp[b^2/2]}\right]. \tag{22}$$

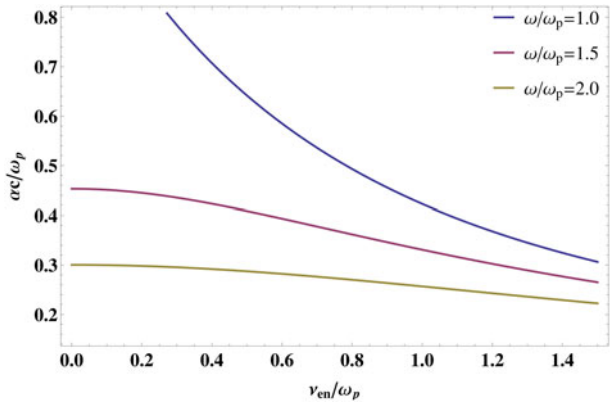

Fig. 2. Plot of the normalized ripple factor $\alpha c/\omega_p$ as a function of the normalized collisional frequency υ_{en}/ω_p at different normalized terahertz frequency ω/ω_p.

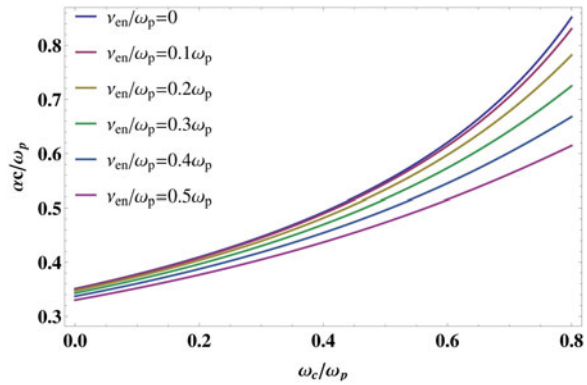

Fig. 3. Plot of the normalized ripple factor $\alpha c/\omega_p$ as a function of the normalized cyclotron frequency ω_c/ω_p at different normalized collisional frequency υ_{en}/ω_p.

Analytical result and discussion

The numerical calculations have been performed for a picosecond CO_2 laser and the following laser–plasma parameters: wavelength $\omega_L = 1.866\times10^{14}$rad/s ($\lambda_L = 10.1\mu$m), laser beam waist size $r_0 = 30\mu$m, laser intensity $I_L = 1.20\times10^{15}$W/cm^2 ($E_L = 9.55\times10^8$V/cm), and plasma electron density $n_0 = 7.561\times10^{16}$ cm^{-3} ($\omega_p = 1.555\times10^{13}$rad/s).

In this model, resonant condition for excitation of THz radiation in Eq. (16) is calculated. As earlier, we said that the density ripple with periodicity $2\pi/\alpha$ is required to be present in the plasma. Hence, $\alpha c/\omega_p$ represents the normalized wave number corresponding to the density ripples. From Eq. (16), the normalized wave number of ripple density $\alpha c/\omega_p$ as a function of normalized collisional frequency υ_{en}/ω_p for different values of THz frequency is plotted in Figure 2. We observe that when we increase the value of collisional frequency, the normalized periodicity of ripple required to efficiently generate the THz radiation at beat wave frequency $\omega/\omega_p = 1.0$ decreases, whereas at higher value of beat wave frequency, the normalized periodicity of ripples required for efficient THz generation remains more or less constant. This implies that at higher beat wave frequency, the THz generation becomes less sensitive to ripple frequency. So, at a given beat wave frequency $\omega/\omega_p \geq 2.0$, one will obtain THz radiation for very large range of collision frequency, provided the ripple frequency is kept at an optimum value. At a lower beat wave frequency, efficient THz generation will be possible for a given combination of α and ν_{en}.

The normalized wave number of ripple density $\alpha c/\omega_p$ as a function of normalized cyclotron frequency ω_c/ω_p for different values of collisional frequency is shown in Figure 3. It is observed that the normalized ripple wave number required for THz generation increases with increasing magnetic field (i.e. ω_c). The lower collisional frequency ν_{en} of plasma (i.e. a higher plasma temperature) requires higher ripple wave number. For the enhanced THz radiation generation, the wavenumber plays a crucial role so static axially magnetic field can be used to tune for strong THz radiation generation.

Now we study the combined effect of cosh-Gaussian laser beams and collisional frequency on THz radiation generation. In Figure 4, we have plotted the generated normalized THz amplitude as a function of normalized beat wave frequency (THz frequency). These plots are generated for two different values of normalized collisional frequency and four different values of decentered parameter b at normalized cyclotron frequency $\omega_c/\omega_p = 0.3$ ($B_0 = 264$kG). The peak of THz amplitude always comes at a resonance condition $\omega \approx (\omega_c^2+\omega_p^2)^{1/2}$ irrespective of the laser profile.

As shown in Figure 4, with the increase in the value of decentered parameter, the normalized THz amplitude increases and is two order higher for hollow-Gaussian beam ($b = 5$) as compared

https://doi.org/10.1017/S0263034618000216 Published online by Cambridge University Press

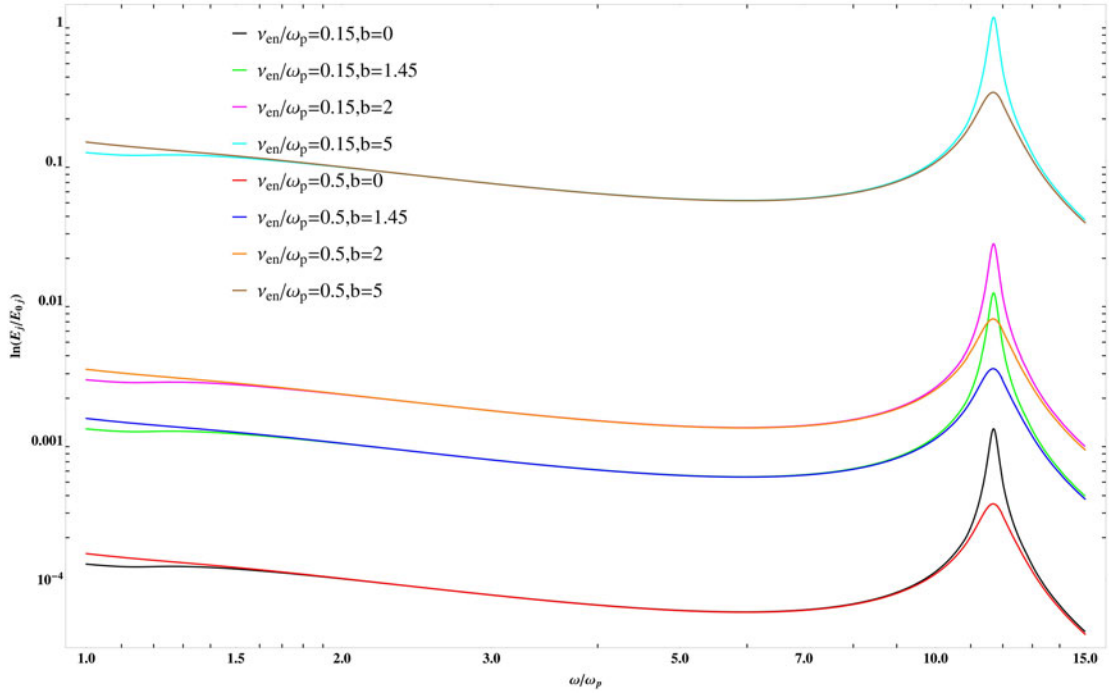

Fig. 4. Plot of the normalized terahertz amplitude $\ln(E_{THz}/E_{01})$ as a function of the normalized terahertz frequency ω/ω_p at different normalized collisional frequency υ_{en}/ω_p and decentered parameter b.

with Gaussian beam ($b = 0$) as the decentered parameter increases, the Gaussian beam peak initially becomes flat-top and then splits into two pulselets in space. This leads to enhanced ponderomotive non-linearity thereby leading to strong non-linear currents and strong THz radiation. Here, we also observe that the peak of normalized THz amplitude increases by few times when collision frequency goes down, that is, plasma is hotter. It is pertinent to mention here that the THz radiation amplitude shows a peak behavior for the magnetized plasma. Using these results, one can change the collision frequency of the plasma and/or magnetic field strength to obtain maximum THz radiation generation. The strength of the magnetic field can be easily tuned by changing the electric current in a solenoid. The collision frequency depends on the electron temperature T_e through the relation $\upsilon_{en} = \upsilon_0(T_e/T_0)^{s/2}$, where s is the collision parameter characterizing the type of collision and T_0 is the electron temperature (Sodha *et al.*, 1974). Thus, by changing the electron temperature, one can tune the collision frequency.

The resonance condition for THz yield is predominantly controlled by magnetic field (ω_c) for phase-matching condition of $\vec{\omega}$ and by ripple frequency (α) for phase-matching condition of $\vec{k}$. For our values of $\omega_c/\omega_p = 0.3$ and $\alpha c/\omega_p = 0.3$, we observe from Figure 4 that at normalized beat wave frequency $\omega/\omega_p = 11.8$, that is, a THz frequency ($\upsilon_{THz} = 11.8$), we obtain a peak for every decentered parameter (b) and collision frequency. The amplitude of peak decreases and the full-width half-maxima (FWHM) increases with increasing the value of collisional frequency. The appearance of peak in the THz yield is due the resonance of beat wave frequency and plasma frequency under the effect of applied magnetic field (B_0) and density ripples. In Figure 5, we show the effect of normalized collisional frequency on normalized THz amplitude and FWHM of the peaks in Figure 4. At $\omega/\omega_p = 11.8$, the normalized THz amplitude decreases with increasing the value of normalized collisional frequency, while the value of FWHM increase. This shows that to generate a shop peak of higher amplitude of THz, one needs lower collision frequency of plasma, that is, a warm plasma.

Now, we study the effect of decentered parameter (b) in the presence of a fixed magnetic field $B_0 = \omega_c m/e$ and fixed ripple frequency on the shape and magnitude of generated THz field amplitude. Figure 6 shows the normalized THz amplitude as a function of beat wave frequency at different values of decentered parameter b. The cyclotron frequency $\omega_c/\omega_p = 0.8$ and normalized ripple factor $\alpha c/\omega_p = 0.3$ have been kept at a constant value. It is seen that, with the increasing value of decentered parameter, the magnitude of emitted THz radiation field increases significantly. The change in magnitude is of three orders from a pure Gaussian beam to a hollow-Gaussian beam.

In Figure 7, the normalized THz field amplitude versus normalized beat wave frequency at different cyclotron frequency (i.e. magnetic field) and same decentered parameter have been plotted. As cyclotron frequency increases the THz amplitude increases and peak shift toward lower value of THz beat wave frequency due to the resonance condition $(\omega_c^2 + \omega_p^2)^{1/2}$. Thus, the peak appearing in the THz amplitude can be tuned by changing axially magnetic field value at a particular THz frequency.

Figure 8 shows that the efficiency η_{THz} of the present scheme increases with cyclotron frequency ω_c/ω_p and decreases with laser beam width (a_0). Efficiency ~15% is achieved by beating of two hollow-Gaussian laser beams at beam width $a_0 \sim c/2\omega_p = 10\mu m$ and magnetic field $\omega_c/\omega_p = 0.8$, which is better than the results reported earlier. For instance, Sheng *et al.* (2004) have obtained an efficiency of about 0.05% for THz emission using inhomogeneous plasma. Malik and Malik (2012) have reported the efficiency of about 0.2% by beating of two spatial-Gaussian lasers. Varshney *et al.* (2013) by using two x-mode lasers in a magnetized plasma have obtained an efficiency of about 1.5%. The maximum reported efficiency belongs to

https://doi.org/10.1017/S0263034618000216 Published online by Cambridge University Press

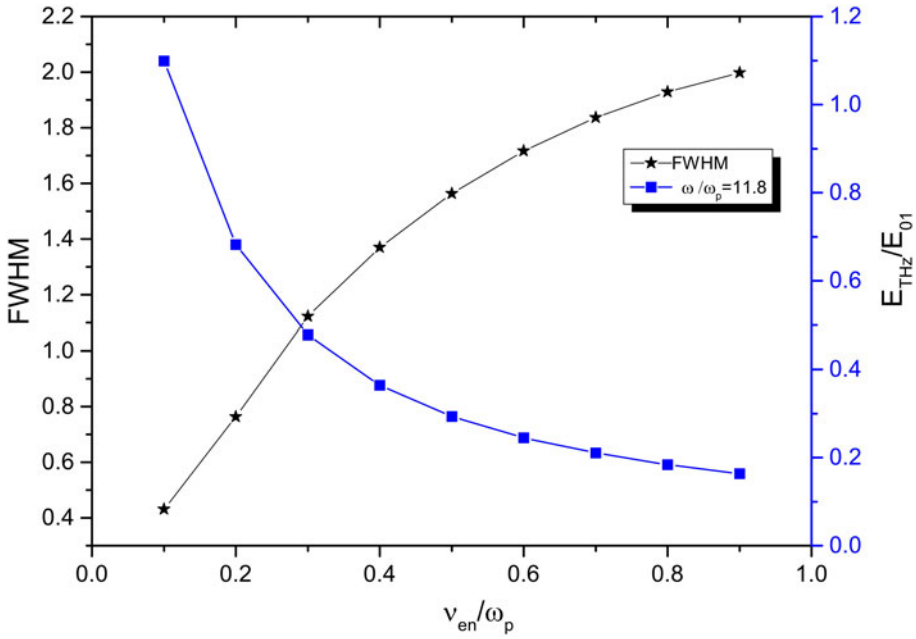

Fig. 5. Plot of the normalized terahertz amplitude E_{THz}/E_{01} and FWHM of terahertz wave as a function of the normalized terahertz frequency υ_{en}/ω_p at normalized terahertz frequency $\omega/\omega_p = 11.8$.

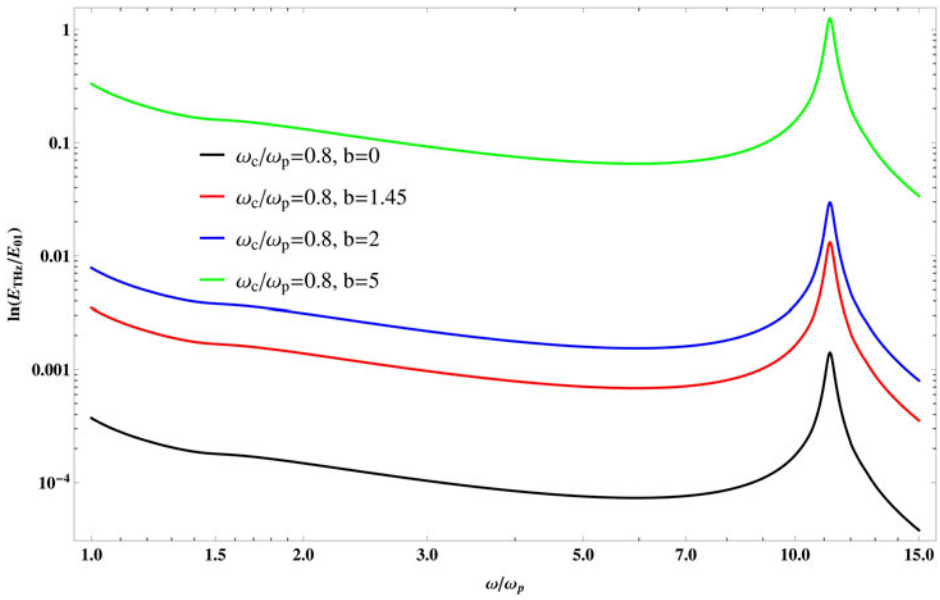

Fig. 6. Plot of the normalized terahertz amplitude $\ln(E_{THz}/E_{01})$ as a function of the normalized terahertz frequency ω/ω_p at different decentered parameter b.

the work done by Singh and Malik (2014) and Bakhtiari *et al.* (2015b) in which the efficiency equal to 5.8% and 8.3% has been obtained, respectively. Thus, the present scheme can produce the THz radiation with high efficiency if the cosh-Gaussian lasers of higher decentered parameter (b) and small beam width (r_0) are used.

Conclusions

We have proposed a model for the generation of THz radiation with high THz amplitude and high efficiency by using two cosh-Gaussian laser beams in axially magnetized rippled plasma. We have also considered the effect of electron-neutral collisions on THz generation. We have derived analytical equations for the electric field amplitude of THz and efficiency of THz radiation and then determined the resonance condition for THz radiation. We have found that the THz field amplitude and efficiency of THz radiation gets enhanced drastically in the magnetized plasma relative to the non-magnetized one. In non-magnetized plasma, the THz field amplitude and efficiency of THz radiation are very small, and they decrease considerably due to the electron-neutral collisions. In magnetized plasma, the negative consequences of electron-neutral collisions can be overcome by a magnetic field. In addition, the joint effect of the magnetic field and electron-neutral collisions causes a further enhancement of THz field amplitude and efficiency when the collision frequency is sufficiently low. This may be due to improved phase--matching condition and tunability due to magnetic field and plasma temperature. By optimizing the applied magnetic field, ripple frequency in plasma, laser beam parameters, and considering

https://doi.org/10.1017/S0263034618000216 Published online by Cambridge University Press

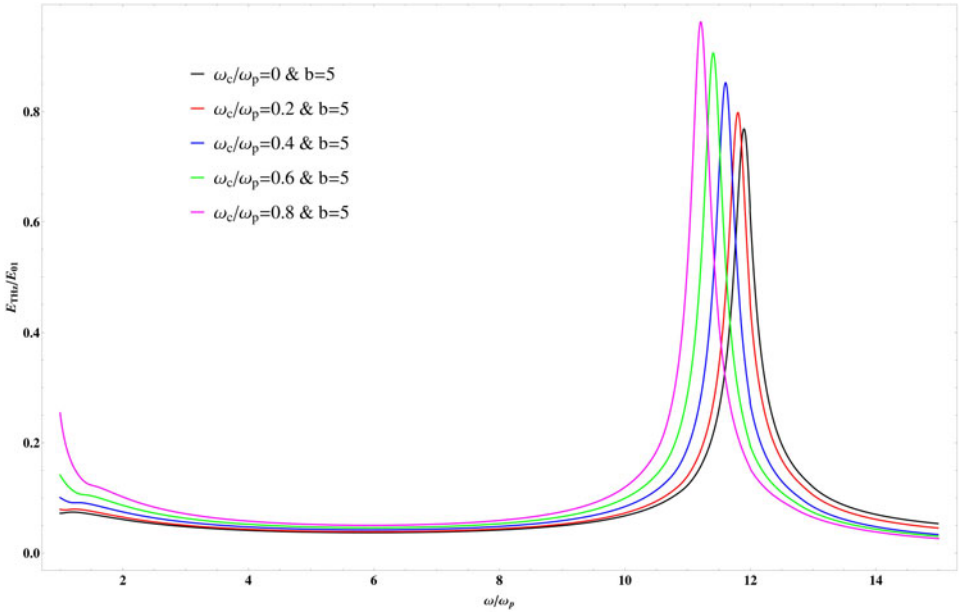

Fig. 7. Plot of the normalized terahertz amplitude E_{THz}/E_{01} as a function of the normalized terahertz frequency ω/ω_p at different normalized cyclotron frequency ω_c/ω_p.

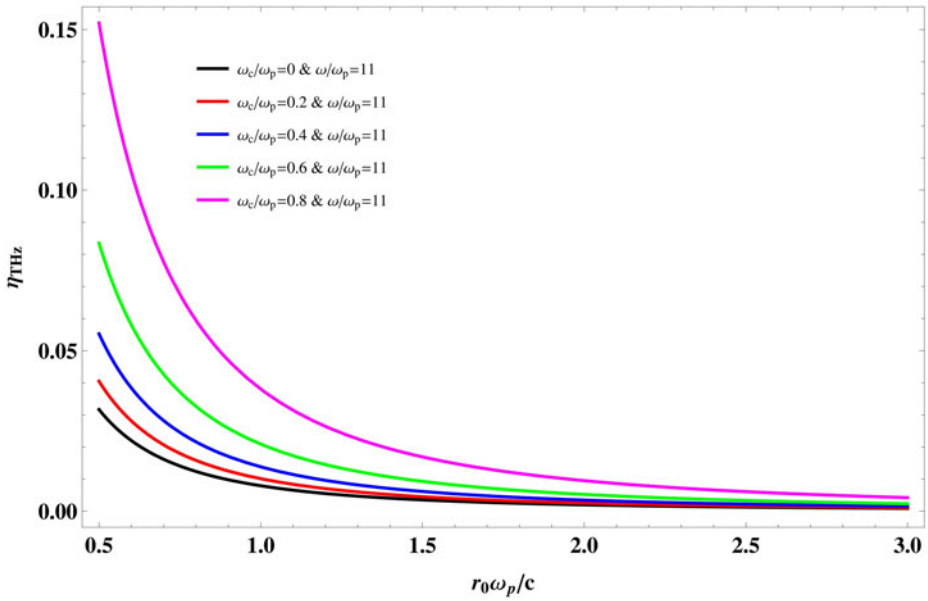

Fig. 8. Plot of the THz efficiency η_{THz} as a function of normalized laser beam waist width $r_0\omega_p/c$ at different values of normalized cyclotron frequency ω_c/ω_p.

the beating, we demonstrate the THz radiation efficiency of up to ~15%. Finally, we have compared the THz radiation generated by hollow-Gaussian and Gaussian laser beams, and we have found that the THz radiation generated by hollow-Gaussian beams has three orders higher amplitude as compared with that generated by Gaussian laser beams, the efficiency of THz generated is five times higher in the case of hollow Gaussian beams.

References

Antonsen Jr TM, Palastro J and Milchberg HM (2007) Excitation of terahertz radiation by laser pulses in nonuniform plasma channels. *Physics of Plasmas (1994–Present)* **14**, 033107.

Babushkin I, Kuehn W, Köhler C, Skupin S, Bergé L, Reimann K, Woerner M, Herrmann J and Elsaesser T (2010a) Ultrafast spatiotemporal dynamics of terahertz generation by ionizing two-color femtosecond pulses in gases. *Physical Review Letters* **105**, 053903.

Babushkin I, Skupin S and Herrmann J (2010b) Generation of terahertz radiation from ionizing two-color laser pulses in Ar filled metallic hollow waveguides. *Optics Express* **18**, 9658–9663.

Bakhtiari F, Esmaeilzadeh M and Ghafary B (2017) Terahertz radiation with high power and high efficiency in a magnetized plasma. *Physics of Plasmas* **24**, 073112.

Bakhtiari F, Golmohammady S, Yousefi M, Kashani FD and Ghafary B (2015a) Generation of terahertz radiation in collisional plasma by beating of two dark hollow laser beams. *Laser and Particle Beams* **33**, 463–472.

Bakhtiari F, Yousefi M, Golmohammady S, Jazayeri SM and Ghafary B (2015b) Generation of terahertz radiation by beating of two circular flattopped laser beams in collisional plasma. *Laser and Particle Beams* **33**, 713–722.

Bass M, Franken P, Ward J and Weinreich G (1962) Optical rectification. *Physical Review Letters* **9**, 446.

Beard MC, Turner GM and Schmuttenmaer CA (2002) Terahertz spectroscopy. *The Journal of Physical Chemistry B* **106**, 7146–7159.

https://doi.org/10.1017/S0263034618000216 Published online by Cambridge University Press

Bhasin L and Tripathi V (2009) Terahertz generation via optical rectification of x-mode laser in a rippled density magnetized plasma. *Physics of Plasmas (1994–Present)* **16**, 103105.

Biedron SG, Lewellen JW, Milton SV, Gopalsami N, Schneider JF, Skubal L, Li Y, Virgo M, Gallerano GP and Doria A (2007) Compact, high-power electron beam based terahertz sources. *Proceedings of the IEEE* **95**, 1666–1678.

Carr GL, Martin MC, Mckinney WR, Jordan K, Neil GR and Williams GP (2002) High-power terahertz radiation from relativistic electrons. *Nature* **420**, 153–156.

Chen FF and Trivelpiece A (1976) Introduction to plasma physics. *Physics Today* **29**(10), pp. 54. https://doi.org/10.1063/1.3024417

Chen Y, Yamaguchi M, Wang M and Zhang X-C (2007) Terahertz pulse generation from noble gases. *Applied Physics Letters* **91**, 251116.

Cho MH, Kim YK, Suk H, Ersfeld B, Jaroszynski DA and Hur MS (2015) Strong terahertz emission from electromagnetic diffusion near cutoff in plasma. *New Journal of Physics* **17**, 043045.

Cook D and Hochstrasser R (2000) Intense terahertz pulses by four-wave rectification in air. *Optics Letters* **25**, 1210–1212.

Dai J, Xie X and Zhang X-C (2006) Detection of broadband terahertz waves with a laser-induced plasma in gases. *Physical Review Letters* **97**, 103903.

Dragoman D and Dragoman M (2004) Terahertz fields and applications. *Progress in Quantum Electronics* **28**, 1–66.

Federici JF, Schulkin B, Huang F, Gary D, Barat R, Oliveira F and Zimdars D (2005) THz imaging and sensing for security applications – explosives, weapons and drugs. *Semiconductor Science and Technology* **20**, S266.

Ferguson B, Wang S, Gray D, Abbott D and Zhang X (2002) Towards functional 3D T-ray imaging. *Physics in Medicine and Biology* **47**, 3735.

Ferguson B and Zhang X-C (2002) Materials for terahertz science and technology. *Nature Materials* **1**, 26–33.

Gill R, Singh D and Malik HK (2017) Multifocal terahertz radiation by intense lasers in rippled plasma. *Journal of Theoretical and Applied Physics* **11**, p. 103 https://doi.org/10.1007/s40094-017-0249-9

Globus T, Woolard D, Bykhovskaia M, Gelmont B, Werbos L and Samuels A (2003) THz-frequency spectroscopic sensing of DNA and related biological materials. *International Journal of High Speed Electronics and Systems* **13**, 903–936.

Hamster H, Sullivan A, Gordon S and Falcone R (1994) Short-pulse terahertz radiation from high-intensity-laser-produced plasmas. *Physical Review E* **49**, 671.

Hamster H, Sullivan A, Gordon S, White W and Falcone R (1993) Subpicosecond, electromagnetic pulses from intense laser-plasma interaction. *Physical Review Letters* **71**, 2725.

Houard A, Liu Y, Prade B, Tikhonchuk VT and Mysyrowicz A (2008) Strong enhancement of terahertz radiation from laser filaments in air by a static electric field. *Physical Review Letters* **100**, 255006.

Hu B and Nuss M (1995) Imaging with terahertz waves. *Optics Letters* **20**, 1716–1718.

Kadow C, Jackson A, Gossard A, Matsuura S and Blake G (2000) Self-assembled ErAs islands in GaAs for optical-heterodyne THz generation. *Applied Physics Letters* **76**, 3510–3512.

Kawase K, Sato M, Taniuchi T and Ito H (1996) Coherent tunable THz-wave generation from LiNbO3 with monolithic grating coupler. *Applied Physics Letters* **68**, 2483–2485.

Kim K-Y, Taylor A, Glownia J and Rodriguez G (2008) Coherent control of terahertz supercontinuum generation in ultrafast laser–gas interactions. *Nature Photonics* **2**, 605–609.

Kumar M, Bhasin L and Tripathi V (2010) Resonant beat wave excitation of terahertz radiation in a magnetized plasma channel. *Physica Scripta* **81**, 045504.

Kumar M, Lee K, Hee Park S, Uk Jeong Y and Vinokurov N (2017) Terahertz radiation generation by nonlinear mixing of two lasers in a plasma with density hill. *Physics of Plasmas* **24**, 033104.

Liu C and Tripathi V (2009) Tunable terahertz radiation from a tunnel ionized magnetized plasma cylinder. *Journal of Applied Physics* **105**, 013313.

Liu Y, Houard A, Prade B, Akturk S, Mysyrowicz A and Tikhonchuk V (2007) Terahertz radiation source in air based on bifilamentation of femtosecond laser pulses. *Physical Review Letters* **99**, 135002.

Löffler T, Jacob F and Roskos H (2000) Generation of terahertz pulses by photoionization of electrically biased air. *Applied Physics Letters* **77**, 453–455.

Malik AK and Malik HK (2013) Tuning and focusing of terahertz radiation by DC magnetic field in a laser beating process. *IEEE Journal of Quantum Electronics* **49**, 232–237.

Malik AK, Malik HK and Kawata S (2010) Investigations on terahertz radiation generated by two superposed femtosecond laser pulses. *Journal of Applied Physics* **107**, 113105.

Malik AK, Malik HK and Stroth U (2011) Strong terahertz radiation by beating of spatial-triangular lasers in a plasma. *Applied Physics Letters* **99**, 071107.

Malik AK, Malik HK and Stroth U (2012) Terahertz radiation generation by beating of two spatial-Gaussian lasers in the presence of a static magnetic field. *Physical Review E* **85**, 016401.

Malik HK (2015) Terahertz radiation generation by lasers with remarkable efficiency in electron–positron plasma. *Physics Letters A* **379**, 2826–2829.

Malik HK and Malik AK (2011) Tunable and collimated terahertz radiation generation by femtosecond laser pulses. *Applied Physics Letters* **99**, 251101.

Malik HK and Malik AK (2012) Strong and collimated terahertz radiation by super-Gaussian lasers. *EPL (Europhysics Letters)* **100**, 45001.

Malik KH (2014) Density bunch formation by microwave in a plasma-filled cylindrical waveguide. *EPL (Europhysics Letters)* **106**, 55002.

Malik R, Uma R and Kumar P (2017) Two color laser driven THz generation in clustered plasma. *Physics of Plasmas* **24**, 073109.

Mann KL, Sajal V, Varshney P and Sharma NK (2017) Terahertz radiation generation by pulse slippage of cosh-Gaussian lasers in a corrugated magnetized plasma. *Physics of Plasmas* **24**, 123117.

Mondal S, Hafez HA, Ropagnol X and Ozaki T (2017) MV/cm terahertz pulses from relativistic laser-plasma interaction characterized by nonlinear terahertz absorption bleaching in n-doped InGaAs. *Optics Express* **25**, 17511–17523.

Nafil RQ, Singh M, Al-Janabi A and Sharma R (2013) THz generation by the beating of two high intense laser beams. *Journal of Plasma Physics* **79**, 657–660.

Pai C-H, Huang S-Y, Kuo C-C, Lin M-W, Wang J, Chen S-Y, Lee C-H and Lin J-Y (2005) Fabrication of spatial transient-density structures as high-field plasma photonic devices. *Physics of Plasmas (1994–Present)* **12**, 070707.

Pathak VB, Dahiya D and Tripathi V (2009) Coherent terahertz radiation from interaction of electron beam with rippled density plasma. *Journal of Applied Physics* **105**, 013315.

Rawat P, Rawat V, Gaur B and Purohit G (2017) Generation of terahertz radiation by intense hollow Gaussian laser beam in magnetised plasma under relativistic-ponderomotive regime. *Physics of Plasmas* **24**, 073113.

Rothwell EJ and Cloud MJ (2008) *Electromagnetic*, 2nd edition, CRC Press, Taylor and Francis Group, Boca Raton, p. 211.

Sakai K (2005) *Terahertz Optoelectronics*. Springer, Berlin, pp. 63–98.

Sharma R, Monika A, Sharma P, Chauhan P and Ji A (2010) Interaction of high power laser beam with magnetized plasma and THz generation. *Laser and Particle Beams* **28**, 531–537.

Sharma R and Singh RK (2014) Terahertz generation by two cross focused laser beams in collisional plasmas. *Physics of Plasmas (1994–Present)* **21**, 073101.

Shen Y-C (2011) Terahertz pulsed spectroscopy and imaging for pharmaceutical applications: a review. *International Journal of Pharmaceutics* **417**, 48–60.

Sheng Z-M, Wu H-C, Li K and Zhang J (2004) Terahertz radiation from the vacuum-plasma interface driven by ultrashort intense laser pulses. *Physical Review E* **69**, 025401.

Singh D and Malik HK (2014) Terahertz generation by mixing of two super-Gaussian laser beams in collisional plasma. *Physics of Plasmas* **21**, 083105.

https://doi.org/10.1017/S0263034618000216 Published online by Cambridge University Press

Singh D and Malik KH (2015) Enhancement of terahertz emission in magnetized collisional plasma. *Plasma Sources Science and Technology* **24**, 045001.

Singh M, Mahmoud S and Sharma R (2012) Generation of THz radiation from laser beam filamentation in a magnetized plasma. *Contributions to Plasma Physics* **52**, 243–250.

Singh M, Singh RK and Sharma RP (2013) THz generation by cosh-Gaussian lasers in a rippled density plasma. *EPL (Europhysics Letters)* **104**, 35002.

Singh RK and Sharma R (2014) Terahertz generation by two cross focused Gaussian laser beams in magnetized plasma. *Physics of Plasmas (1994-present)* **21**, 113109.

Singh RK, Singh M, Rajouria SK and Sharma R (2017) Strong terahertz emission by optical rectification of shaped laser pulse in transversely magnetized plasma. *Physics of Plasmas* **24**, 073114.

Sodha MS, Ghatak AK and Tripathi VK (1974) *Self-Focusing of Laser Beams in Dielectrics, Plasmas and Semiconductors*. Tata McGraw-Hill Pub. Co. New Delhi, p. 81.

Tripathi D, Bhasin L, Uma R and Tripathi V (2010) Terahertz generation by an amplitude-modulated Gaussian laser beam in a rippled density plasma column. *Physica Scripta* **82**, 035504.

Varshnety P, Sajal V, Chauhan P, Kumar R and Sharma NK (2014) Effects of transverse static electric field on terahertz radiation generation by beating of two transversely modulated Gaussian laser beams in a plasma. *Laser and Particle Beams* **32**, 375–381.

Varshney P, Sajal V, Baliyan S, Sharma NK, Chauhan PK and Kumar R (2015a) Strong terahertz radiation generation by beating of two x-mode spatial triangular lasers in magnetized plasma. *Laser and Particle Beams* **33**, 51–58.

Varshney P, Sajal V, Singh KP, Kumar R and Sharma NK (2013) Strong terahertz radiation generation by beating of extra-ordinary mode lasers in a rippled density magnetized plasma. *Laser and Particle Beams* **31**, 337–344.

Varshney P, Sajal V, Singh KP, Kumar R and Sharma NK (2015b) Tunable and efficient terahertz radiation generation by photomixing of two super Gaussian laser pulses in a corrugated magnetized plasma. *Journal of Applied Physics* **117**, 193303.

Varshney P, Sajal V, Upadhyay A, Chakera JA and Kumar R (2017) Tunable terahertz radiation generation by nonlinear photomixing of cosh-Gaussian laser pulses in corrugated magnetized plasma. *Laser and Particle Beams* **35**, 279–285.

Wang S, Ferguson B, Abbott D and Zhang X-C (2003) T-ray imaging and tomography. *Journal of Biological Physics* **29**, 247–256.

Wang T-J, Ju J, Liu Y, Li R, Xu Z and Leang Chin S (2017) Waveform control of enhanced THz radiation from femtosecond laser filament in air. *Applied Physics Letters* **110**, 221102.

Zeitler JA, Taday PF, Newnham DA, Pepper M, Gordon KC and Rades T (2007) Terahertz pulsed spectroscopy and imaging in the pharmaceutical setting-a review. *Journal of Pharmacy and Pharmacology* **59**, 209–223.

https://doi.org/10.1017/S0263034618000216 Published online by Cambridge University Press